# User-Friendly Simulator for Estimating Power Consumption and Communication Availability in Wireless Sensor Networks

Yuta Hosokawa, Yuki Ogawa, Ryuta Nakasone, Minoru Tanaka, and Kazuki Nakamura
Information and Communication Technology Division
Railway Technical Research Institute
Kokubunji, Tokyo, 185-8540 Japan
e-mail: {hosokawa.yuta.84, ogawa.yuki.87, nakasone.ryuta.07, tanaka.minoru.96, nakamura.kazuki.26}@rtri.or.jp

***Abstract*—In railway infrastructure monitoring, wireless sensor networks (WSNs) offer considerable potential for collecting sensor data at locations where communication cables and/or power lines cannot be installed. However, for practical adoption, railway operators must design networks that maintain communication reliability while minimizing the maintenance costs, particularly for battery replacement. In this study, we introduced simulation models that predict communication performance and power consumption in WSNs. The proposed simulation model was implemented as a user-friendly, web-based tool. The simulator enables railway operators to compare various network configurations without requiring specialized technical knowledge. To validate the simulation models, we constructed an actual WSN along a test railway line. The experimental results indicated that the simulator provides highly accurate estimations of the data arrival rates and power consumption, demonstrating the effectiveness of the approach. Thus, the proposed simulator supports cost-effective deployment and reduced maintenance effort in railway environments where wire-based sensing of infrastructure is impractical.**

***Keywords*—monitoring; power consumption; railway; simulator; wireless sensor network.***

## I. INTRODUCTION

This study builds upon our preliminary work presented at The Eighteenth International Conference on Sensor Technologies and Applications (SENSORCOMM 2024) [1], where we introduced the concept of a web-based simulator for the deployment of wireless sensor networks (WSNs). We extend the findings of the previous work by obtaining parameters in real-world settings and validating the proposed models using the actual equipment installed in a railway environment.

In recent years, Japanese railway operators have increasingly sought to adopt more efficient and labor-saving technologies for the maintenance of railway equipment. One approach is to use WSNs to remotely monitor equipment distributed along the railway lines. Using WSNs can reduce the frequency of on-site inspections; however, the following elements must be considered when applying this principle: communication range, modulation method, power consumption, and power supply implementation. These elements interact with each other, and the variety of available options renders the design of optimal WSNs challenging for railway operators.

Several types of network simulators have been developed for WSN design. Sharma et al. [2] conducted a comprehensive comparative analysis of the WSN simulation frameworks, while highlighting their merits and demerits based on key characteristics such as scalability, graphical support, and ease of implementation. Idris et al. [3] surveyed the available Internet of Things (IoT) and WSN simulation tools for long-range wide-area network (LoRaWAN) [4] to demonstrate the evolving landscape of network simulation tools. These comparative analyses reveal the trade-offs between simulation flexibility and practical usability, wherein existing simulators typically prioritize accuracy and research depth over operational accessibility.

General-purpose simulators such as Network Simulator-2 (ns-2) [5], Network Simulator-3 (ns-3) [6], and OMNeT++ [7] provide flexible discrete-event simulation platforms for network research. These tools can be used to model various network types, ranging from wired networks to wireless sensor networks. In particular, ns-3 supports power consumption modeling through extensions such as Energy Framework [8]. A WSN-specific module Castalia [9] was developed for OMNeT++. More recently, the INET Framework [10] provided extensions for simulating WSNs, including radio propagation and power consumption models. The ns-2, ns-3, and OMNeT++ are open-source simulators, whereas QualNet [11] is a commercial network simulator that provides high-fidelity models and supports a wide range of wireless technologies. QualNet has been widely used in both academia and industry. Furthermore, it has been integrated into EXata [12], a real-time network emulation platform that inherits the detailed protocol models of QualNet while focusing on real-time network emulation capabilities. However, substantial programming expertise (typically in C++) and a deep understanding of simulation are essential for using these simulators.

Protocol-specific simulators typically focus on particular communication methods and provide detailed analysis for specific protocols. For example, LoRaSim [13] is a Python-based simulator that models large-scale LoRa networks using an analytically derived physical layer model. It focuses on evaluating the scalability and packet collisions in dense deployments, thereby enabling researchers to determine the change in network performance with an increase in the number of LoRa nodes. Another simulator, LoRaWANSim [14], was implemented in MATLAB that offers comprehensive LoRaWAN simulation from the physical layer

to the application layer. MATLAB-based tools present several advantages in terms of rapid prototyping and visualization, making them accessible to engineers familiar with numerical computing. Although these simulators excel at protocol-level performance evaluation, their single-protocol focus limits their utility when comparing multiple communication methods.

Development-integrated platforms such as Contiki-NG [15] provide an operating system for IoT devices combined with the Cooja simulation environment [16], enabling developers to test the same application code on both simulated and real hardware. This framework enables users to simulate the behavior of embedded devices without modifying the code. Although this approach is beneficial for protocol development and debugging, it requires programming expertise in C and embedded systems.

Overall, these simulators typically require advanced technical expertise for command-line operations, custom scripting, or detailed parameter configuration. Conversely, there is extensive demand from non-technical users of railway operators to rapidly evaluate the possible WSN configurations among the various available options. Therefore, conventional, highly detailed network simulators are typically unsuitable for railway operators, as their complexity makes rapid, practical evaluation difficult for non-experts in wireless networking.

To address these issues, we propose a user-friendly simulator to estimate the communication quality and battery consumption of WSNs in railway environments. The proposed simulator supports multi-hop transmission and mesh networking for nodes that extend over long distances along the railways. It features a web-based graphical user interface (GUI), which enables users to set parameters easily, compare node placements and communication methods, and instantly view the results. The simulator satisfies the specific requirements of WSN deployment planning in railway maintenance operations without requiring specialized software or technical expertise.

The remainder of this paper is organized as follows. Section II presents the proposed simulation framework. Section III describes in detail the experimental characterization of the WSN technologies, including the radio propagation properties and power consumption behavior. Section IV presents a detailed explanation of the development of the simulation models. Section V describes the implementation of the web-based simulator. Section VI presents the verification of the simulator using actual WSN deployments along a test railway line. Section VII details a practical case study that depicts the implementation of the simulator in WSN design under realistic constraints. Finally, Section VIII concludes the paper.

## II. Proposed Simulation Framework

In railway environments, WSN deployment requires operators to evaluate node placement, communication methods, and battery replacement schedules corresponding to specific monitoring targets and deployment sites. To meet these requirements, we developed a comprehensive simulation framework to evaluate the communication quality and power consumption of wireless sensors designed

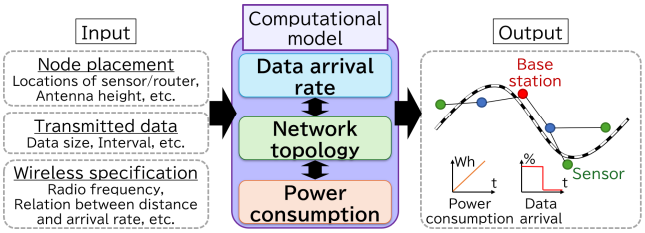


Figure 1. Overview of the proposed simulation framework.

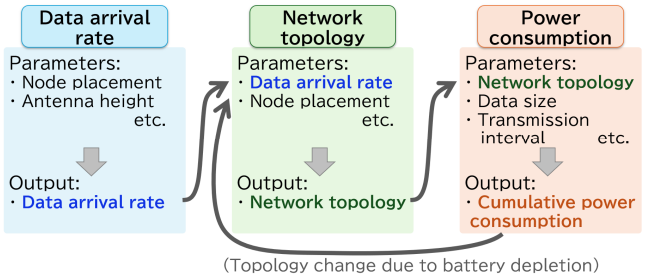


Figure 2. Relationship of the three estimation models.

specifically for the railway infrastructure constraints and operational requirements.

Figure 1 shows the overall architecture of the proposed simulation method. This framework accepts three types of input parameters: node placement information, including wireless sensor locations, and site characteristics; data transmission specifications, such as the payload size and transmission intervals; and wireless specifications. The computational model performs a WSN simulation based on these inputs and outputs power consumption profiles and data arrival rates for each network node.

The computational model comprises three interconnected estimation models: data arrival rate estimation, network topology estimation to determine the data transmission paths, and power consumption estimation. These models operate cooperatively to conduct a comprehensive network simulation (Figure 2).

The proposed framework adopts a feedback mechanism, wherein the output from each estimation model is fed into subsequent models to create an integrated simulation loop that captures dynamic network interactions. This interconnected approach enables the realistic modeling of the network behavior under various operational conditions.

Additionally, modeling the topology reconfiguration based on battery depletion events is a crucial feature of the proposed framework. When the power consumption estimation indicates node battery exhaustion, this information is propagated back to the network topology estimation model, which recalculates optimal routing paths for the modified network. This iterative process continues throughout the simulation, presenting a realistic prediction of long-term network evolution and maintenance requirements.

Furthermore, the proposed framework comprises various WSN architectures, ranging from simple star topologies, as typically employed in LoRaWAN, to complex mesh networks, commonly observed in wireless smart ubiquitous networks

(Wi-SUN) [17] deployments. This flexibility enables the implementation of the proposed framework in various railway monitoring applications. Moreover, the modular architecture facilitates adaptation to different communication protocols by replacing individual estimation models, while preserving the integrity of the overall simulation framework.

Existing network simulators require specialized technical knowledge and command-line expertise. Conversely, the proposed framework prioritizes practical usability for railway operators. The simulation provided immediate feedback on crucial deployment parameters, thereby enabling rapid design iteration and network optimization prior to physical implementation.

## III. Experimental Characterization of WSN Technologies

To establish estimation models for communication performance and power consumption, we conducted field experiments using Wi-SUN and LoRa devices.

### A. Target Technology Selection and Measurement Approach

The appropriate selection of frequency bands and communication protocols is crucial in WSN deployment, particularly for railway applications with unique operational constraints. We established the following specific selection criteria: communication range capabilities of several kilometers, battery operation sustainability for multiple years, and license-free operation in Japan, enabling railway operators to independently construct private networks. These requirements ensure the practical applicability of railway infrastructure monitoring while maintaining operational autonomy.

Based on these criteria and their widespread implementation in WSN deployments in Japanese railways, we selected Wi-SUN and LoRa as the target protocols for comprehensive characterization. The complementary characteristics of these protocols, i.e., the reliability of Wi-SUN and the exceptional range of LoRa, render them well-suited for railway monitoring scenarios. We performed targeted baseline measurements using the aforementioned technologies. These measurements are not intended to be universally applicable across all wireless systems; instead, they reflect the specific conditions corresponding to railway applications.

#### 1) Frequency Band Selection

The protocol selection adopted in this study focused on specific low-power radio stations operating without radio station licenses in Japan. Among the available frequency bands (e.g., 429 MHz, 920 MHz, and 2.45 GHz), we selected the 920 MHz band for its optimal balance of communication range, data rate, and power efficiency. Although the 920 MHz band presents a shorter range than the 429 MHz band, it provides superior data rates and multi-hop transmission. When compared with the 2.45 GHz band, it sacrifices speed for a significantly longer range and lower power consumption, which are critical factors for battery-operated railway sensors.

#### 2) Protocol Characteristics

##### a) Wi-SUN

Wi-SUN is an IEEE802.15.4g-compliant protocol that is widely employed in smart meter applications. Despite the higher standby current (tens of mA) when compared with other LPWA technologies, Wi-SUN delivers communication speeds of several hundred kbps over distances up to 1 km. Its field area network (FAN) profile provides robust mesh networking with automatic route reconfiguration during node failures, thereby ensuring high network reliability for critical railway monitoring applications.

##### b) LoRa

LoRa employs chirp spread spectrum modulation to achieve exceptional power efficiency and transmission range. It excels in remote monitoring scenarios owing to standby currents as low as 0.7 μA and communication distances extending 1–10 km. Although the LoRaWAN typically employs star topologies, private LoRa configurations support multi-hop networking, thereby providing deployment flexibility for the linear railway infrastructure.

The complementary characteristics of these protocols render them essential for different railway monitoring scenarios, justifying their selection for comprehensive characterization.

### B. Radio Propagation Characteristics

We systematically measured the RSSI and data arrival rates across various inter-node distances to establish reliable communication feasibility criteria for the proposed simulation framework. For target communication ranges of several kilometers, we conducted experiments on a straight viaduct, which provides the 3 km straight sections required for long-range testing.

The experimental setup involved fixing a base station and moving a remote unit to various distances while measuring the RSSI and data arrival rates at each location. Figure 3 shows the experimental configuration employed in this study. We configured the transmission power at 20 mW, representing the maximum allowable output for the 920 MHz-specified low-power radio stations in Japan, with a standardized payload size

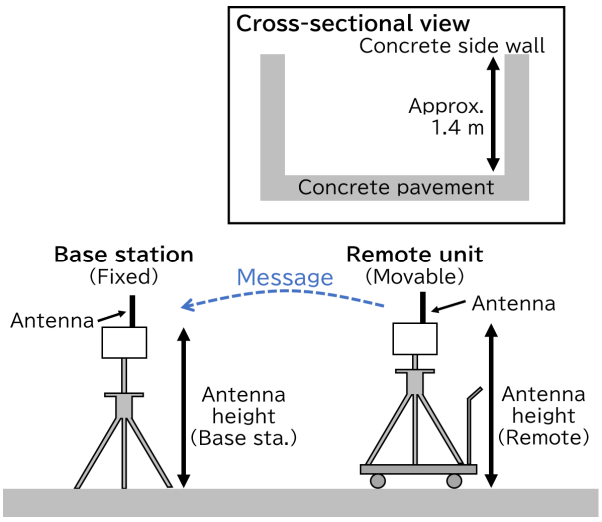


Figure 3. Experimental setup for radio propagation test.

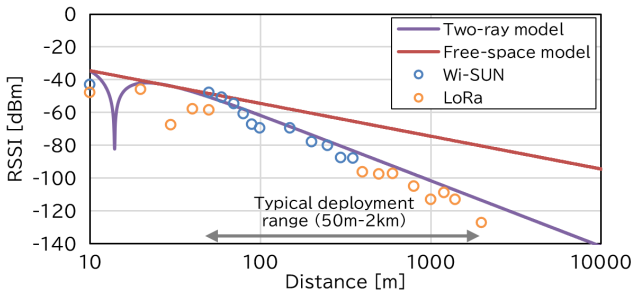


Figure 4. Relationship between distance and RSSI.

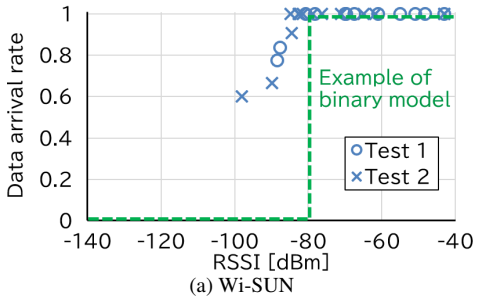


(a) Wi-SUN

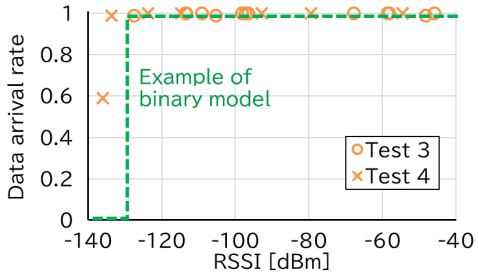


(b) LoRa

Figure 5. Relationship between RSSI and data arrival rate.

of 16 bytes per transmission. The testing conditions included multiple antenna height configurations and both Wi-SUN and LoRa protocols to ensure comprehensive characterization.

**Measurement Results:** Figure 4 shows the relationship between antenna distance and RSSI. The measurement results indicated that both the Wi-SUN and LoRa protocols exhibit similar distance-dependent RSSI characteristics under identical antenna and power configurations. In particular, in the range 50 m to 2 km, which represents that of typical WSN deployment scenarios, the measured values closely concurred with the two-ray ground-reflection model [18] predictions rather than free-space propagation models.

Consequently, we adopted the two-ray ground-reflection model as the foundation for our simulation framework. This model assumes a flat ground surface with a clear line-of-sight path between the nodes. It characterizes radio propagation by considering the interference between the direct path and the ground-reflected path. It is particularly advantageous for railway environments, where communication nodes are typically arranged along linear tracks on flat terrain or elevated viaducts. However, it does not account for the additional attenuation or interference caused by railway

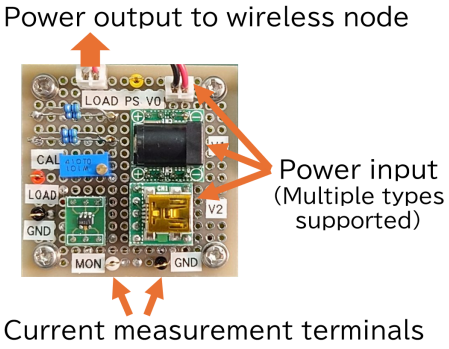


Figure 6. Custom circuit for current detection.


Figure 7. Commercial USB tester.

infrastructure, such as utility poles, overhead power lines, tunnels, or station structures.

Figure 5 shows the relationship between the RSSI and data arrival rates. The results demonstrated a characteristic threshold behavior for both protocols. Above certain RSSI thresholds, both the Wi-SUN and LoRa maintained arrival rates exceeding 99%. However, the arrival rates decreased rapidly when the RSSI fell below these thresholds, indicating that a binary threshold-based model (binary model) was appropriate for simulation.

### C. Power Consumption Characterization

Measurement of power consumption presents unique challenges for the characterization of wireless sensors. Voltage monitoring requires a simple parallel connection, whereas current measurement requires series insertion of measurement equipment into the power path. This requirement was addressed using two complementary approaches: a custom current detection circuit for module-level measurement (Figure 6) and a commercial USB tester for system-level characterization (Figure 7).

The current detection circuit developed in this study enables insertion between the wireless sensor modules and power supplies, presenting a voltage output proportional to the consumed current. This approach enables a detailed oscilloscope-based analysis of the instantaneous power consumption patterns. Additionally, we selected and validated the AVHzY CT-3 USB tester [19], which demonstrated a measurement accuracy with an error within 1% at 1000 samples per second while providing continuous data logging capabilities.

**Measurement Results:** The characterization of power consumption revealed distinct operational states for both the Wi-SUN and LoRa modules, with consumption varying significantly between the sleep, standby, and transmission

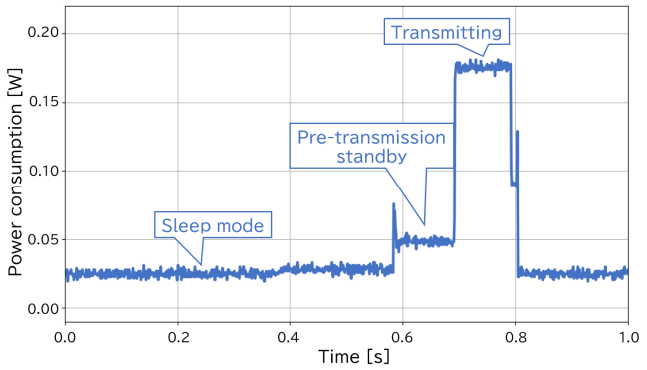


(a) Wi-SUN

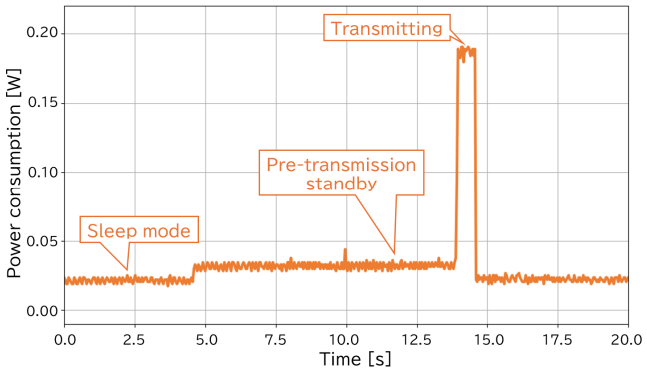


(b) LoRa

Figure 8. Example results of power consumption.

phases. Figure 8 shows the representative power consumption waveforms for both the protocols, demonstrating the power consumption profiles during different operational phases. As expected, the transmission duration and the associated power consumption scaled with the data payload size, thereby requiring multiple measurement scenarios to establish the representative power models.

These measurement data present the parameters required for the power consumption estimation model of the proposed simulation framework. An analysis of the power consumption profiles indicates that the node power consumption can be effectively modeled using two representative states. This includes the waiting state, which dominates the overall operation time when the node is not actively transmitting data, and the transmitting state, which exhibits the highest instantaneous power consumption. In this study, we refer to the non-transmitting periods, including sleep or reception standby, as the waiting state. This two-state approximation ensures that the essential power consumption behavior is captured while maintaining the computational efficiency for simulation. However, these results represent specific hardware configurations used in validation testing. Practical deployment requires the characterization of the actual target hardware to ensure accurate power consumption prediction.

## IV. Simulation Model Development

The simulation framework employed the three interconnected models highlighted in Section II: data arrival rate estimation, network topology determination, and power consumption prediction models. These models operate cooperatively to capture the real-world network dynamics including topology reconfiguration due to battery depletion.

### A. Data Arrival Rate Estimation Model

The data arrival rate estimation model determines the communication feasibility between the node pairs based on their positioning and transmission parameters. For the Wi-SUN and LoRa protocols operating in the 920 MHz band under clear line-of-sight conditions with inter-node distances within 2 km, the relationship between communication distance and RSSI closely follows the two-ray ground-reflection model predictions, as described in Section III. B.

Our measurements demonstrated a clear threshold behavior in the RSSI-arrival rate relationship: communication was highly reliable (>99% arrival rate) above certain RSSI values, but deteriorated rapidly below these thresholds.

Therefore, we employed the two-ray ground-reflection model to calculate the RSSI at each node pair for simulation and then compared these values against the predetermined RSSI thresholds to determine the communication feasibility. This approach presents a practical binary decision criterion: communication was considered to be feasible (arrival rate = 100%) when the calculated RSSI exceeded the threshold and infeasible (arrival rate = 0%) otherwise.

The two-ray ground-reflection model estimation formula based on the inter-node distance was expressed as follows:

$$P_{rx} = P_{tx} - L_{tx} + G_{tx} + G_{rx} - L_{rx} + 20\log_{10}\frac{\lambda \times \left|\sin\frac{2\pi h_{tx} h_{rx}}{\lambda d}\right|}{4\pi d}. \quad (1)$$

$$\begin{pmatrix} d\text{: Distance between the nodes[m]} \\ \lambda\text{: Wavelength [m]} \\ P_{tx}\text{: Transmission power [dBm]} \\ P_{rx}\text{: Received power [dBm]} \\ G_{tx}\text{: Transmitting node antenna gain [dBi]} \\ G_{rx}\text{: Receiving node antenna gain [dBi]} \\ L_{tx}\text{: Cable and filter loss of transmitting node [dB]} \\ L_{rx}\text{: Cable and filter loss of receiving node [dB]} \\ h_{tx}\text{: Transmitting node antenna height [m]} \\ h_{rx}\text{: Receiving node antenna height [m]} \end{pmatrix}$$

Figure 9 shows an example wherein seven nodes were placed, and the communication availability between the nodes was estimated using the aforementioned procedure. The yellow dashed lines represent the communication-available links, and the numbers represent the estimated RSSI values.

### B. Network Topology Estimation Model

The network topology estimation model determined the optimal transmission paths when there were multiple routing options between the sensor nodes and the base station. We employed the routing protocol for low-power and lossy networks (RPL), which was widely adopted in Wi-SUN and similar multi-hop networks, to autonomously establish these transmission paths. Our implementation follows the standard RPL procedure, which is given as follows:

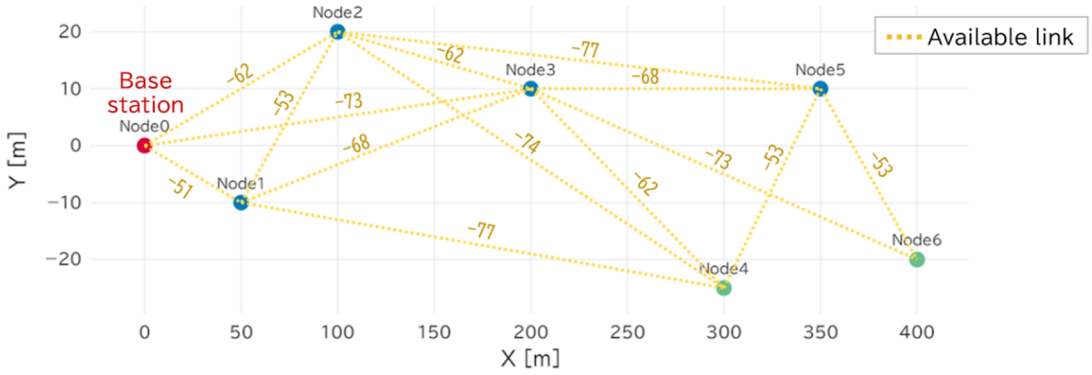


Figure 9. Example of communication availability estimation.

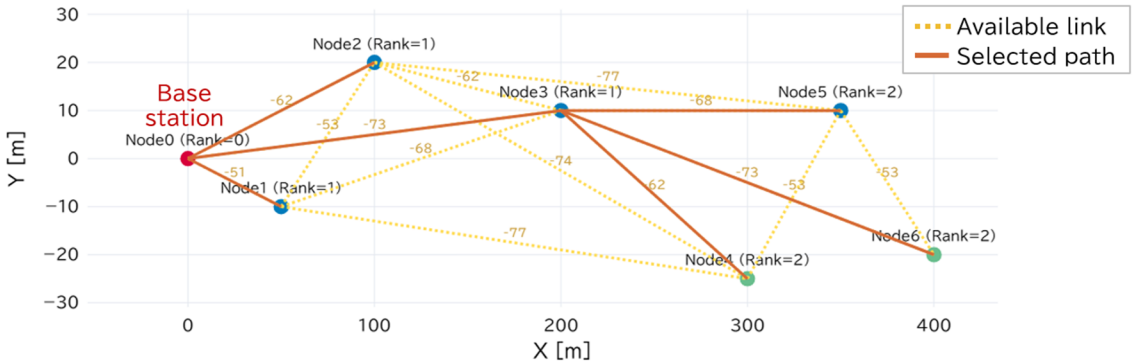


Figure 10. Example of network topology estimation.

1) We assigned a Rank value of 0 to the base station, where Rank represents the hop count required to reach the base station.
2) We assigned a Rank of 1 to the nodes capable of direct communication with the base station, with direct routes established to the base station.
3) We assigned a Rank of 2 to nodes that can communicate with nodes of Rank 1, but lack established routes. When there are multiple parent candidates, the algorithm selects the route with the highest estimated RSSI.
4) This process was repeated iteratively, assigning a Rank of k+1 to the nodes communicating with nodes with Rank k until all the nodes have established routes.

Figure 10 shows example results of estimating the transmission paths from each node to the base station, assuming the node configuration shown in Figure 9. This implementation ensured optimal parent selection based on signal strength, while minimizing hop counts to the base station. The modular design enabled the substitution of alternative routing algorithms to support different multi-hop protocols beyond Wi-SUN.

### C. Power Consumption Estimation Model

The power consumption model estimated the battery consumption for each battery-powered node using a simplified two-state approach based on the measurement results obtained in this study. The wireless sensor power consumption varied significantly across operational phases, with the largest differences occurring between the waiting and active transmission periods, as described in Section III. C. Figure 11 shows the employed power consumption model.

The proposed model simplified this behavior into two primary states: a waiting state consuming $P_{wait}$ [W] and a transmitting state consuming $P_{tx}$ [W]. These parameters were configured based on the node functionality. Sensor nodes (leaf nodes), which only collect and transmit the sensor data, can utilize sleep mode while waiting to minimize the power consumption. Conversely, the router nodes must maintain a constant standby operation to receive and relay data from the

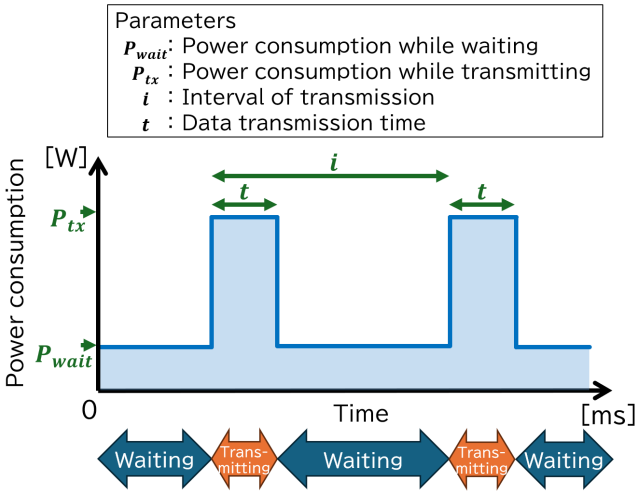


Figure 11. Power consumption model [1].

other nodes, thereby presenting higher power consumption during the waiting state ($P_{wait}$). The transmission duration scaled linearly with the data payload size. In the proposed model, this relationship was expressed as $t = ax + b$, where $x$ [Bytes] denotes the size of the transmitted data. Each node transmits data at its configured transmission interval $i$ [s]. In multi-hop networks, router nodes must relay the data received from child nodes in addition to transmitting their own sensor data, presenting higher power consumption.

The cumulative power consumption was calculated by integrating these power states over time and generating battery consumption predictions for each network node. This enables the evaluation of battery replacement schedules and identification of nodes requiring higher-capacity batteries or an external power supply. The proposed modeling approach captures the essential WSN operational dynamics while maintaining the computational efficiency required for real-time network design evaluation.

## V. IMPLEMENTATION

We developed a simulator for WSNs that considers both data transmission and power consumption. The simulator was implemented in Python 3.11 using an open-source Python library called the Streamlit [20] library to enable web-based GUI controls. It was developed on a Linux server in our local network, enabling users to interact with it via a web browser on any PC connected to the network. Figure 12 shows a sample screen of the interface of the proposed simulator. The simulator comprised the following three components:

### A. *Parameter input interface*

The simulator provides a web-based interface for users to input all the required parameters, including the node placement, characteristics, and battery capacity. The interface features real-time updates, where variations in the input values are instantly reflected in the corresponding graphs, facilitating rapid iteration of the simulation parameters.

### B. *Network and Communication Path Visualization*

The simulator generates a visual representation based on the input parameters, which depicts the

- Node placement
- Inter-node communication availability
- Data transmission routes from each node to the base station

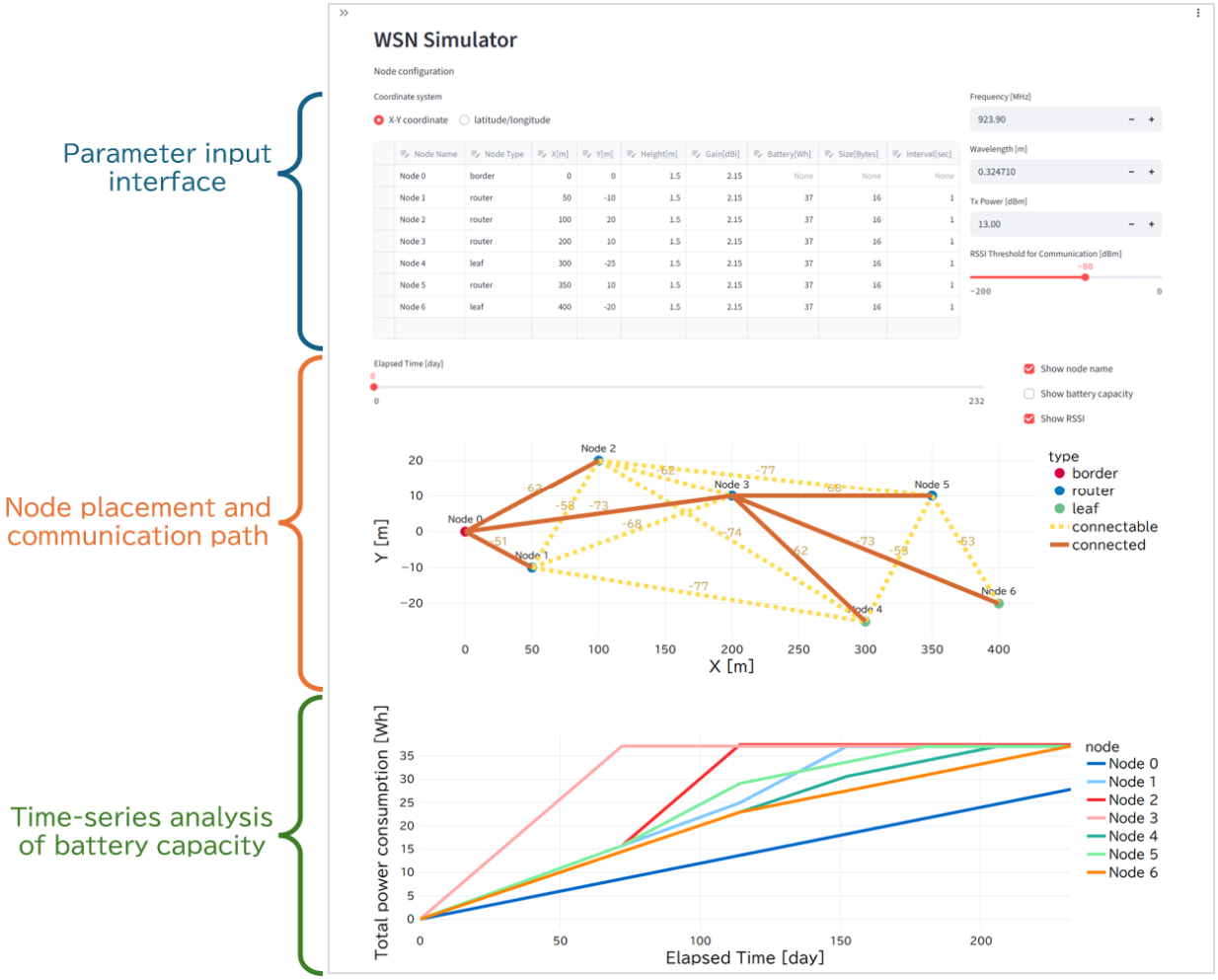


Figure 12. Screenshot of the developed simulator.

A dynamic timeline feature enables users to simulate the battery consumption over time. This includes dynamic re-routing when the nodes deplete their batteries.

### C. Time-series analysis of battery capacity

The simulator presents a graph that depicts the relationship between the elapsed time and cumulative power consumption for each node. The key features are as follows:

- Simulation is continued until the entire battery capacity is depleted.
- Time resolution can be selected as one day, one hour, or one minute, allowing users to optimize the simulation for planning battery replacement strategies in WSN deployments.
- Visualization of long-term network behavior in scenarios without battery replacement is feasible.

## VI. VERIFICATION

To demonstrate that the proposed simulator accurately reflects the behavior of a WSN implemented with actual devices, we constructed a Wi-SUN-based WSN along a test railway line at the Railway Technical Research Institute and compared the results with those obtained from the simulator. The experiments were conducted to demonstrate the following: (1) reproduction of the network topology and reflection of changes in topology when the battery capacity of a node runs out; (2) accuracy of data arrival rate estimation, and (3) accuracy of power consumption estimation.

### A. Experimental Setup

Figure 13 shows the node placement in the verification experiments. We installed wireless sensor nodes based on the 920 MHz Wi-SUN standards at these locations (Figure 14). Each router and sensor node periodically collected the environmental data. In particular, the temperature, humidity, and atmospheric pressure data were obtained and transmitted wirelessly to the base station. The sensor node was placed far away and could not communicate directly with the base station. Consequently, the data transmission paths were established using the RPL, thereby enabling multi-hop communication via intermediate router nodes. We employed ROHM's Wi-SUN communication modules (model: BP35C5-T01).

We artificially increased the size of the transmitted data to accelerate battery consumption and complete the verification experiments within a reasonable time frame. Although real-world sensor data would only contain a few bytes, we appended random data to enlarge each packet to 256 bytes. Furthermore, we configured a short transmission interval of one second, which was considerably more frequent than in the typical use cases, to emphasize the power consumption model.

### B. Verification of Network Topology and Arrival Rate Simulation

Figure 15 presents the simulation results of the data transmission path obtained by executing the simulator with the node placement and corresponding parameters depicted in Figure 13. The orange lines in the figure represent the selected transmission path, which was determined using the network

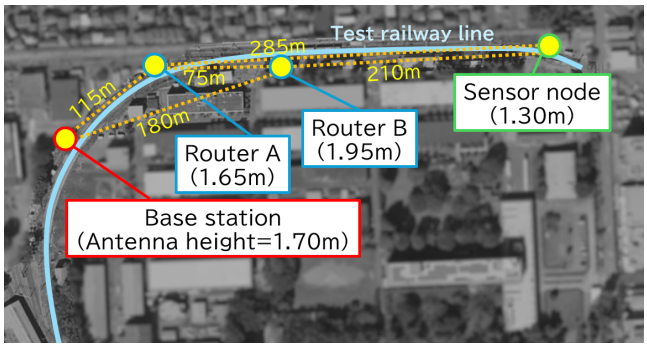


Figure 13. Node placement in the experiments (modified from an aerial photograph provided by the Geospatial Information Authority of Japan [21]).

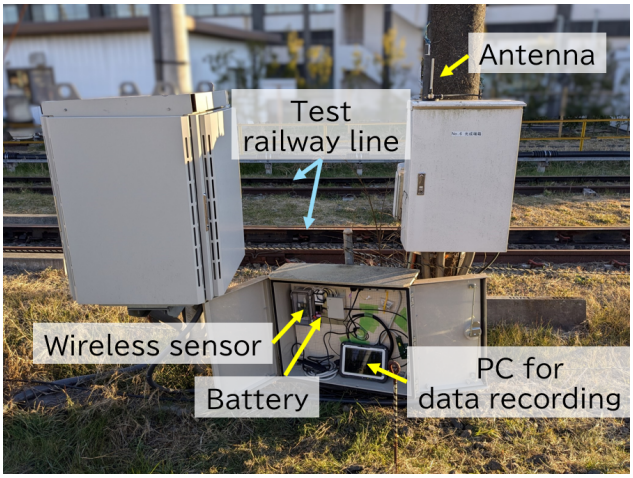


Figure 14. Wireless sensor node deployed along the test railway line.

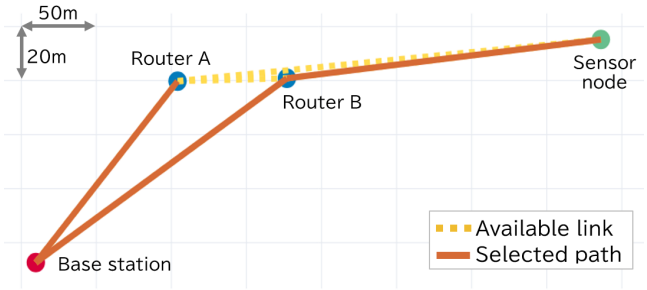


(a) Initial transmission path

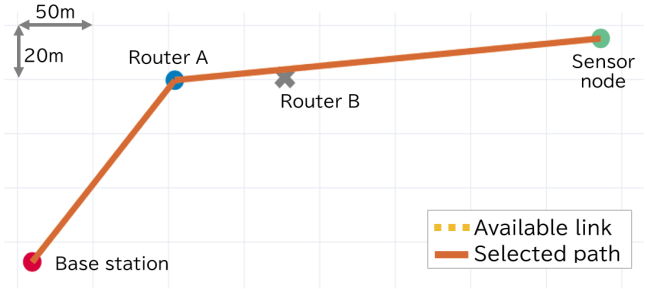


(b) Transmission path after router B became unavailable

Figure 15. Simulation results of the transmission path.

TABLE I. MEASURED RESULTS OF RSSI AND DATA ARRIVAL RATE

| Link | RSSI [dBm] (Estimated) | RSSI [dBm] (Measured Avg.) | Arrival Rate (Estimated) | Arrival Rate (Measured) |
|---|---|---|---|---|
| Sensor node → Router B | -73 | -76.82 | 100% | 99.97% (286657/286738) |
| Router B → Base station | -67 | -73.62 | 100% | 100.00% (295314/295318) |
| Router A → Base station | -61 | -66.63 | 100% | 100.00% (295145/295154) |

topology estimation model described in Section IV. B. Direct transmission could not be achieved under the test conditions owing to the long distance between the terminal sensor node and the base station. Therefore, the sensor data were initially transmitted via router B. Subsequently, router B experienced battery depletion owing to its relatively high power consumption for relaying operations, presenting a change in the network topology, as shown in the simulation outcome.

We deployed a WSN along the test railway line using the Wi-SUN modules to validate the simulation results. Consequently, the initial network topology matched the simulation output, with the sensor data being transmitted through router B. Furthermore, router B eventually exhausted its battery capacity as time progressed owing to its relaying operations, and the transmission path was shifted to the route via router A (Figure 15 (b)).

Table I presents the measurement results of the RSSI and data arrival rate. The experiment involved continuous data transmission at 1-s intervals over approximately 88 h, totaling approximately 300,000 transmissions. This table lists the average RSSI value and arrival rate for each communication link. The measured RSSI values were up to 6 dB lower than the estimated values. This was attributed to the presence of physical obstacles in the actual environment, such as railway structures and wayside buildings, which were not considered in the simulation that assumed an unobstructed terrain. In particular, the link between router B and the base station likely experienced a deteriorated RSSI owing to the obstruction by wayside buildings (see Figure 13).

Despite these environmental differences, the actual data arrival rates for all the communication links, estimated to be 100% in the simulation, were 99.97% or higher. These results indicated that the estimation error of the simulation model was sufficiently low, thereby demonstrating the practical reliability of the model.

### C. Verification of Power Consumption Simulation

We measured the power consumption of routers A and B, and the sensor node in a WSN deployed along the test railway line to evaluate the accuracy of the simulator in estimating the power consumption. Routers A and B were powered using mobile batteries with a rated capacity of 11.84 Wh. The experiment was continued until the data transmission ceased due to the depletion of the battery capacity.

Figure 16 shows the cumulative power consumption over time for each node. The dashed lines represent the simulation results, whereas the solid lines represent the actual experimental measurements. At the beginning of the

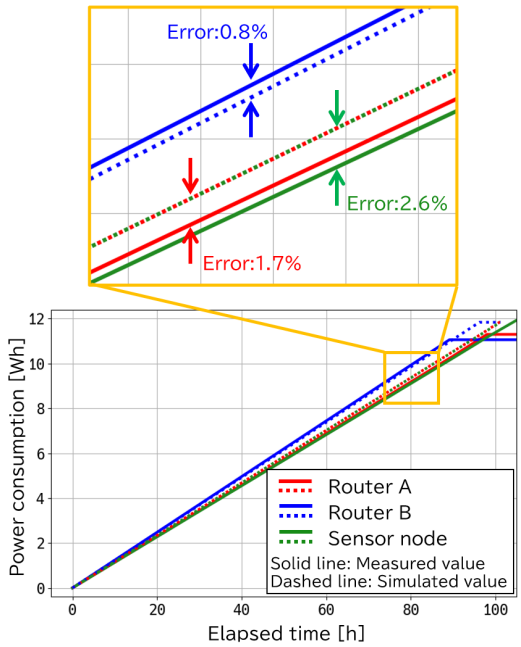


Figure 16. Time-series comparison of simulated and measured cumulative power consumption.

experiment, the data from the sensor node were transmitted via router B (Figure 15(a)). Consequently, router B has to transmit both its own sensor data and that obtained from the sensor node, presenting higher power consumption when compared with router A. As highlighted in the magnified view presented in Figure 16, the estimation error appeared as a difference in the slope of the cumulative power consumption over time, representing the difference in the average power consumption. The operating time until the depletion of the battery capacity was determined by the total energy extracted from the battery, corresponding to the consumption rate. Therefore, we calculated the total energy consumed by each router in the experiment. Table II presents the detailed measurement results.

The maximum error in the estimated power consumption per unit time was 2.6%, demonstrating that the simulator accurately estimated the power consumption of the wireless sensor nodes (Table II). Conversely, the actual-to-rated capacity ratios indicated that the batteries delivered 93.4% to 95.4% of their rated capacity under the test conditions. This

TABLE II. DETAILED MEASUREMENT RESULTS OF POWER CONSUMPTION

| Node | Average power consumption [W] | | |
|---|---|---|---|
| | Estimated value | Measured value | Error rate |
| Router A | 0.117 | 0.115 | 1.7% |
| Router B | 0.123 | 0.124 | 0.8% |
| Sensor node | 0.117 | 0.114 | 2.6% |

| Node | Battery capacity [Wh] | | |
|---|---|---|---|
| | Rated | Measured capacity | Capacity ratio (Actual/Rated) |
| Router A | 11.84 | 11.30 | 95.4% |
| Router B | 11.84 | 11.06 | 93.4% |
| Sensor node | — | — | — |

variation was attributed to factors such as the battery type, degradation level, ambient temperature, and humidity.

### D. Model Limitations and Practical Considerations

Although the proposed simulation models aligned closely with the measurement results, they still face several limitations.

First, the current network topology estimation assumes the use of RPL routing as defined in Wi-SUN FAN. However, the modular design of the simulator enables this component to be replaced with alternative routing algorithms. This flexibility enables future extensions to various communication standards based on the user requirements.

Second, the radio propagation model is based on the two-ray ground-reflection assumption, which assumes a flat ground surface and clear line-of-sight conditions. This model is well-suited for railway environments where nodes are typically deployed along flat, straight railway tracks or elevated viaducts. However, more detailed propagation modeling is required for environments with complex geometries or significant obstructions.

Lastly, the battery consumption model does not consider temperature-dependent characteristics or long-term degradation of battery cells. Although these factors were outside the scope of this work, incorporating them can improve the lifetime estimation accuracy in real deployments.

## VII. Case Study: Applying the Simulator to Real World WSN Design

We conducted a case study on the design process of a WSN to demonstrate the practical utility of the proposed simulator, focusing on how it supports the selection of optimal node configurations and communication methods under realistic constraints. This section describes the procedure, input parameters, and representative results obtained using the proposed simulator.

### A. Simulation Setup and Input Parameters

The simulator requires several key input parameters to accurately model WSN behavior:

#### 1) Node Placement

The geographical positions of the nodes were specified in either latitude/longitude or relative distance coordinates. These positions must be determined based on the actual deployment scenarios in railway environments. The locations of the sensor nodes (where the sensors were to be installed) and the base station (where the sensor data were aggregated) were defined. Additionally, the candidate router locations must also be set as parameters.

#### 2) Wireless Communication Parameters

Wireless characteristics, such as the frequency band and receiver sensitivity (e.g., reception threshold) were configured. These parameters can be derived from actual measurements or datasheets of commercially available devices.

#### 3) Power Consumption Parameters

The power consumption values for both the transmission and waiting states, along with the battery capacity, were specified based on the empirical measurements of the candidate hardware. These values enabled the simulator to estimate the power consumption and battery replacement cycles under different traffic patterns and network topologies.

### B. Example of WSN Design using the Simulator

In an example scenario, four sensor nodes were placed along a hypothetical railway section; they communicated with the central base station via an intermediate router. The initial configuration is shown in Figure 17(a). In this scenario, the router must forward data from all four sensor nodes, resulting in high power consumption and early battery depletion. Figure 17(b) shows the simulation results of power consumption using a 100 Wh battery. The results indicated that the battery lasted for approximately 61 days.

Based on the simulation results, railway operators aim to extend the battery replacement cycles to reduce the cost of maintaining these networks. We analyzed several redesign strategies for extending the battery replacement cycle.

#### 1) Adding an Additional Router Node

The first scenario involved adding another router to reduce the amount of data transmitted by each router node. Figure 18 shows the node placement and simulation results obtained in this case. This approach extended the battery life and increased the battery replacement cycle to 74 days.

#### 2) Changing the Communication Method

The second scenario involved switching from a short-range protocol to a long-range one (e.g., from Wi-SUN to LoRa), which enabled the sensor nodes to bypass the intermediate relays, presenting simpler topologies and reduced energy consumption. Figure 19 shows the node placement and simulation results. This configuration extended the battery replacement cycle to approximately 140 days.

Based on these illustrative scenarios, users can evaluate multiple network design options using the proposed simulator prior to the actual WSN deployment in railway environments. As observed in these examples, the proposed web-based simulator enabled non-specialist users of railway operators to effectively analyze various network design strategies. By

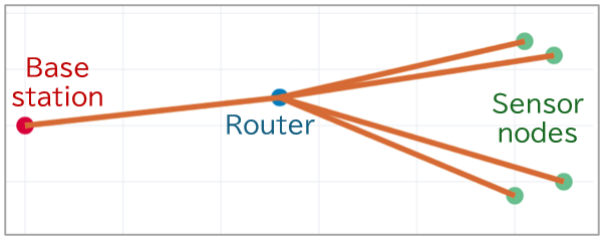


(a) Node placement

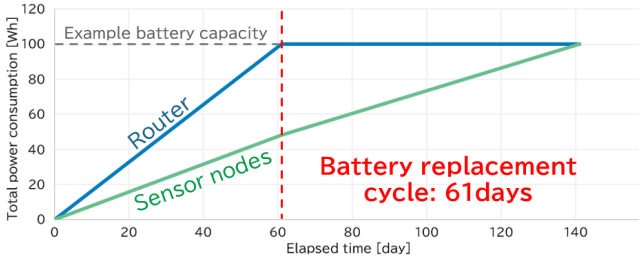


(b) Power consumption simulation results

Figure 17. Example of initial configuration.

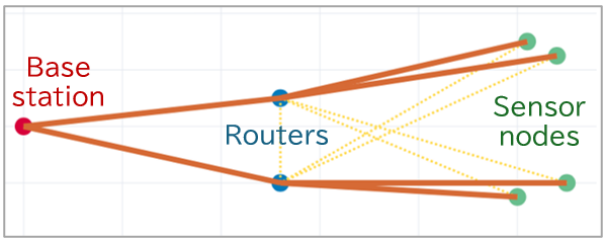


(a) Node placement

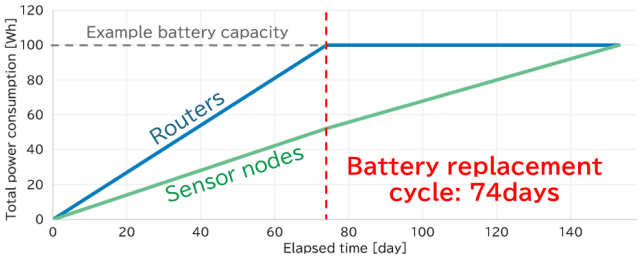


(b) Power consumption simulation results

Figure 18. Adding an additional router node.

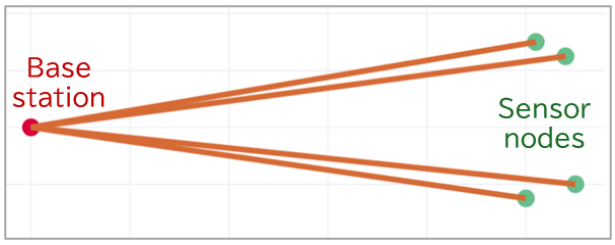


(a) Node placement

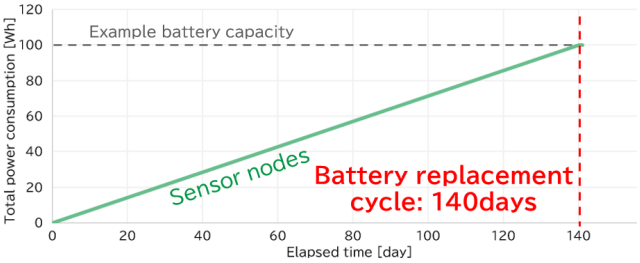


(b) Power consumption simulation results

Figure 19. Changing the communication method.

configuring and comparing different scenarios, such as those presented here, users with minimal technical expertise can make informed decisions regarding hardware selection, node placement, and maintenance plans. The ability to simulate both the communication quality and power consumption significantly reduced the uncertainty and costs associated with WSN deployment in railway environments. Furthermore, the proposed simulator framework enables easy adaptation to other wireless standards and application domains beyond railways.

## VIII. Conclusion

In this study, we proposed a simulation-based approach to support railway operators in designing WSNs. We aimed to provide a practical tool to facilitate network planning without requiring advanced technical expertise. Communication experiments conducted with Wi-SUN and LoRa were used to characterize key parameters—data arrival rate and power consumption—which formed the basis for the modeling. These models were integrated into a user-friendly, web-based simulator capable of estimating the communication availability and power consumption under various deployment conditions. That enabled users to easily compare different node placements and other parameters to satisfy the specific requirements of railway applications.

We conducted validation experiments by constructing a small-scale WSN along the test railway line. The experimental results indicated that the proposed simulator achieves high estimation accuracy for both communication performance and battery usage. The simulator provides a practical and accessible tool for evaluating the WSN configurations in railway environments. It enables non-specialist users to evaluate the network performance under realistic conditions and supports the design of reliable, low-maintenance monitoring systems.

## References

[1] Y. Hosokawa, M. Tanaka, and K. Nakamura, “Easy-to-use wireless sensor network simulator for estimating power consumption and communication availability,” The Eighteenth International Conference on Sensor Technologies and Applications (SENSORCOMM 2024), IARIA, Nov. 2024, pp. 4–7.

[2] R. Sharma, V. Vashisht, and U. Singh, “Modelling and simulation frameworks for wireless sensor networks: a comparative study,” IET Wireless Sensor Systems, vol. 10, no. 5, pp. 181–197, Oct. 2020.

[3] S. Idris, T. Karunathilake, and A. Förster, “Survey and comparative study of LoRa-enabled simulators for internet of things and wireless sensor networks,” Sensors, vol. 22, no. 15, p. 5546, Jul. 2022.

[4] LoRa Alliance: About LoRaWAN. [Online]. Available from: https://lora-alliance.org/about-lorawan/ 2025.12.01

[5] ns-2: The Network Simulator—ns-2. [Online]. Available from: https://www.isi.edu/websites/nsnam/ns/ 2025.12.01

[6] ns-3: A discrete-event network simulator for internet systems. [Online]. Available from: https://www.nsnam.org/ 2025.12.01

[7] A. Varga and R. Hornig, “An overview of the OMNeT++ simulation environment,” Proceedings of the 1st International Conference on Simulation Tools and Techniques for Communications, Networks and Systems & Workshops (Simutools ’08), ICST, Mar. 2008, pp. 1–10.

[8] H. Wu, S. Nabar, and R. Poovendran, “An energy framework for the network simulator 3 (ns-3),” Proceedings of the 4th International ICST Conference on Simulation Tools and Techniques (Simutools ’11), ICST, Mar. 2011, pp. 222–230.

[9] A. Boulis: Castalia: an OMNeT-based simulator for low-power wireless networks such as wireless sensor networks and body area networks. [Online]. Available from: https://github.com/boulis/Castalia/ 2025.12.01

[10] INET Framework. [Online]. Available from: https://inet.omnetpp.org/ 2025.12.01

[11] Keysight Technologies: QualNet Network Simulator. [Online]. Available from: https://www.keysight.com/us/en/assets/3122-1395/technical-overviews/QualNet-Network-Simulator.pdf 2025.12.01

[12] Keysight Technologies: EXata Network Modeling. [Online]. Available from: https://www.keysight.com/us/en/assets/3122-1406/technical-overviews/EXata-Network-Modeling.pdf 2025.12.01

[13] M. C. Bor, U. Roedig, T. Voigt, and J. M. Alonso, "Do LoRa low-power wide-area networks scale?," Proceedings of the 19th ACM International Conference on Modeling, Analysis and Simulation of Wireless and Mobile Systems (MSWiM '16), ACM, Nov. 2016, pp. 59–67.

[14] R. Marini, K. Mikhaylov, G. Pasolini, and C. Buratti, "LoRaWANSim: a flexible simulator for LoRaWAN networks," Sensors, vol. 21, no. 3, p. 695, Jan. 2021.

[15] G. Oikonomou, S. Duquennoy, A. Elsts, J. Eriksson, Y. Tanaka, and N. Tsiftes, "The Contiki-NG open source operating system for next generation IoT devices," SoftwareX, vol. 18, p. 101089, Jun. 2022.

[16] F. Osterlind, A. Dunkels, J. Eriksson, N. Finne, and T. Voigt, "Cross-level sensor network simulation with cooja," Proceedings. 2006 31st IEEE conference on local computer networks (LCN), IEEE, Nov. 2006, pp. 641–648.

[17] R. Hirakawa, K. Mizutani, and H. Harada, "Specification and performance analysis of Wi-SUN FAN," IEEE Open Journal of Vehicular Technology, vol. 4, pp. 849–866, 2023.

[18] W. C. Jakes, Ed., Microwave mobile communications. New York: John Wiley & Sons, Inc., pp. 80–83, 1974.

[19] AVHzY: CT-3 USB 3.1 power meter tester digital multimeter current tester voltage detector lua interpreter integrated DC 26V 6A. [Online]. Available from: https://www.avhzy.com/html/product-detail/ct3/ 2025.12.01

[20] Snowflake: Streamlit, a faster way to build and share data apps. [Online]. Available from: https://streamlit.io/ 2025.12.01

[21] Geospatial Information Authority of Japan (GSI): Map and aerial photo browsing service. [Online]. Available from: https://service.gsi.go.jp/map-photos/app/map?search=photo/ 2025.12.01